

Single IFFT Augmented Spectral Efficiency DMT Transmitter

Qibing Wang⁽¹⁾, Binhuang Song⁽¹⁾, Bill Corcoran⁽¹⁾, Leimeng Zhuang⁽¹⁾, Arthur Lowery⁽¹⁾

⁽¹⁾ Electro-Photonics Laboratory, Department of Electrical and Computer Systems Engineering, Monash University, Clayton, VIC 3800, qibing.wang@monash.edu

Abstract *The computational load for ASE-DMT can be reduced to that of DCO-OFDM by mapping of the inverse fast Fourier transform's (IFFTs) inputs and extraction of signals from within the IFFT. A real-time transmitter enables 9.2 Gbit/s over 20-km SSMF.*

Introduction

Optical orthogonal frequency division multiplexing (OFDM), also known as discrete multi-tone (DMT), is one of the main modulation format candidates in short-haul data centre interconnect to meet the rapidly increasing data traffic¹. Compared with 4-level pulse amplitude modulation, DMT has a better tolerance to fibre dispersion and can adapt its modulation formats of different subcarriers according to the transmission curve via bit-loading and power-loading. Therefore, it is more suitable for medium transmission distances from 10 km to 100 km². However, a large DC bias is required to achieve non-negative laser drive signal in intensity modulation and direct detection (IMDD) based short-haul fibre-optic links. This is not power efficient because the DC bias does not carry information. Because they do not require a DC-bias, asymmetrically clipped optical OFDM (ACO-OFDM)³ and pulse-amplitude-modulated optical DMT (PAM-DMT)⁴ have been proposed to improve the power efficiency of DC-biased optical OFDM (DCO-OFDM), by clipping negative excursions to zero, to achieve unipolar signals. However, these two schemes have to leave the even subcarriers (ACO) or the real parts (PAM) unmodulated; thus, sacrifice half of their spectral efficiency. Layered/enhanced ACO-OFDM (EACO-OFDM)⁵⁻⁸ has been developed to improve the spectral efficiency of ACO-OFDM towards that of DCO-OFDM, while still maintaining a power advantage through clipping, by allowing the even-frequency subcarriers to be used. Similarly, augmented spectral efficiency DMT (ASE-DMT)⁹ uses layering applied to PAM-DMT, by modulating its unused real parts in additional layers. EACO-OFDM transmission experiments using off-line¹⁰ and in-line¹¹⁻¹² digital signal processing (DSP) have been demonstrated, but ASE-DMT has yet to be experimentally demonstrated efficiently.

In this paper, we introduce an efficient method of generating ASE-DMT signals by carefully mapping the layers to the inputs of one IFFT and by extracting the higher layer's waveforms from within the core of the IFFT, so they can be clipped

separately before combination. We demonstrate a FPGA-based ASE-DMT transmitter with a net data rate of 9.2 Gb/s. A Q-factor of 15.2 dB is obtained after 20-km standard single-mode fibre (SSMF) transmission.

ASE-DMT transmitter algorithm

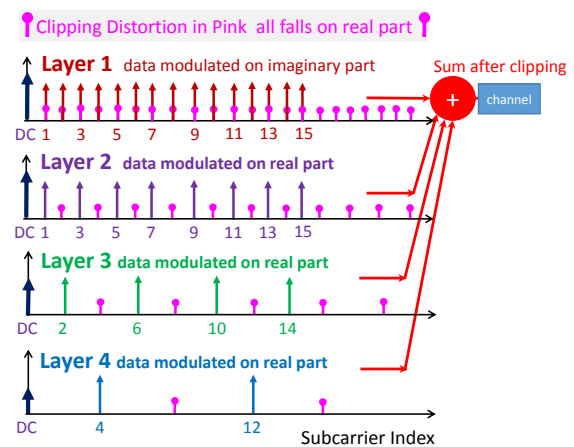


Fig. 1: Data-carrying subcarrier allocations for ASE-DMT.

The signal generation procedure of ASE-DMT is illustrated in Fig. 1. Four layers are used and the spectra of each layer are coloured. In the first layer, the imaginary parts in all subcarriers are pulse amplitude modulated, which is the same as PAM-DMT⁴. The higher layers, L (2, 3, 4), just carry real-valued pulse-amplitude modulation, in a set of subcarriers that have frequency indices $2^{(L-2)}(2n+1)$, where $n = (0, 1, 2, 3, \dots)$. Each layer generates a superposition of its subcarriers using an inverse fast Fourier transform (IFFT); then the negative values of each layer's waveform are clipped to become zero-valued. Finally, the already-clipped waveforms of all layers are combined to achieve a unipolar signal output. Importantly, this scheme guarantees that the clipping distortion from higher layers has no influence on the data-decoding process in the lower layers. Therefore, Layer 1 can be decoded first, using a FFT and a slicer. This data can then regenerate a facsimile of Layer 1's transmitted waveform using an IFFT and a clipper, which is subtracted from the received waveform, to reveal the subcarriers of higher layers. Now Layer 2 becomes free of clipping-distortion, so can be

decoded. The same procedure applies to higher layers until the data in all the layers is recovered. More details of this iterative receiver can be found in these papers⁵⁻⁹.

ASE-DMT transmitter implementation

Islim *et al.* have estimated that the computational complexity of ASE-DMT transmitter is the same as a QAM DCO-OFDM transmitter for the same spectral efficiency, because only the real-valued or the imaginary-valued frames in the ASE-DMT transmitter need be computed, avoiding a complex IFFT⁹. We now experimentally demonstrate that: (a) re-arranging the IFFT's inputs and (b) extracting signals from within the IFFT, reduces the computation of all layers of ASE-DMT to that of one complex IFFT.

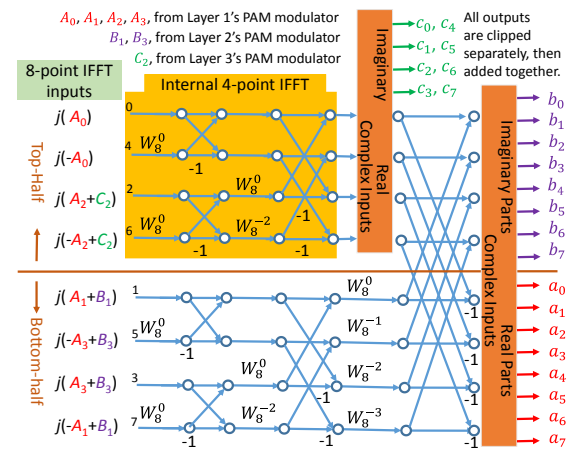


Fig. 2: 8-point radix-2 DIT IFFT butterfly flow chart.

Fig. 2 illustrates how a complex 8-point decimation-in-time (DIT) IFFT butterfly can generate three layers simultaneously. Modification (a) maps the (real) PAM modulator outputs four subcarrier frequencies to the imaginary frequency inputs of the IFFT, based on the idea that one complex-valued IFFT can be used to compute two real-valued FFTs¹³. For example, Layer 1 will only appear on the real outputs if the IFFT's inputs are Hermitian: If the inputs have the same imaginary parts (and opposite real parts, if used), their transforms appear as only imaginary valued at the output.

Modification (b) uses the fact that the top/bottom data flows in the complex DIT-IFFTs are separate except in the final butterfly. Thus, the 4-point IFFT (orange area in Fig. 2) is used for Layer 3, and the bottom flow for Layer 2. The innovation is to extract the IFFT of Layer 3 (c_n) before the final butterfly, so that the outputs of Layers 2 and 3 can be separated. This is achieved by separating the real and imaginary parts of the data just after the 4-point IFFT: the imaginary parts become Layer 3's *real* waveform after the block (c_0, c_1, c_2, c_3) is duplicated⁵. Clipping can be applied before duplication. The real parts of the orange area flow on to the final

butterfly, which calculates the waveforms for Layers 1 and 2. Conveniently, Layer 1 (a_n) is contained in the real parts of the final output and Layer 2 (b_n) is in its imaginary parts. Thus these two waveforms can be separately clipped before summation with Layer 3's clipped waveform. By applying Modification (b) multiple times, systems with more than 3 layers can be implemented.

Fig. 3 shows DSP functions performed in the FPGA in our experimental demonstration. Four layers were implemented using one 128-point IFFT module. The test data and two training symbols were stored in the FPGA. For each clock cycle, 59 data bits were mapped to 59 PAM2 symbols, each with 12-bit resolution. Afterwards, these 59 symbols, combined with their Hermitian counterparts, were distributed to four layers through a data distribution module illustrated in Fig. 2. These 59 PAM2 symbols carry the same data as 28 QPSK-modulated subcarriers and three PAM2-modulated subcarriers, giving 95.2% of the spectral efficiency of DCO-OFDM whose subcarriers (excluding DC) would be all QPSK. In each layer, the 128 12-bit real outputs were then clipped to remove all negative values before being added together. The set-range and quantization module transformed this into 128 5-bit words. Finally, a 32-sample cyclic prefix (CP) was pre-pended to every OFDM symbol, producing 160 positive 5-bit words, which were distributed to 20 high-speed FPGA transmitters, representing four 5-bit parallel data streams to feed the MICRAM DAC. Of the available resources on the Vertix-6 FPGA (XC6VLX240T), the design used 16% of the slice registers (48259), 29% of the slice LUTs (43833) and 100% of the DSP48E1s (768).

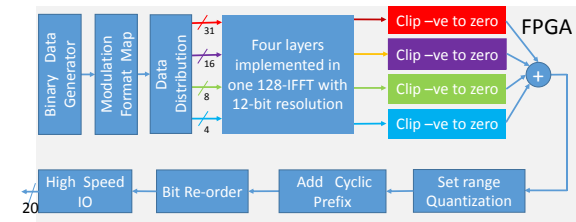


Fig. 3: DSP functions implemented in the FPGA.

Experimental demonstration

Fig. 4 shows the experimental setup. A 156.25-MHz clock generated by the DAC provided a clock to the FPGA, which was used to control all the DSP modules in the FPGA and synchronize the FPGA and DAC. Each high-speed transmitter converted 40 parallel streams from FPGA core fabric to 6.25-Gb/s outputs. In the DAC, every four 6.25-Gb/s signals were further multiplexed to a 25-Gb/s bit stream to generate 6.25-GHz analog signal. Because 59 data bits were encoded and 32-sample CP was appended in one clock, the net data rate was 9.2 Gb/s, neglecting an overhead of two training symbols.

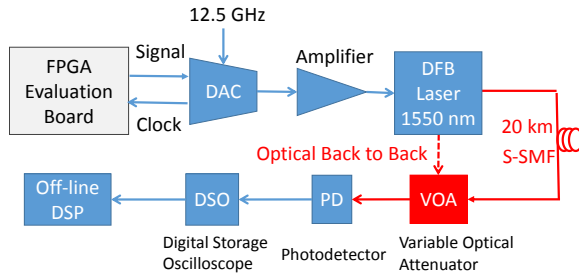


Fig. 4: Experimental setup of the ASE-DMT transmitter.

The DAC's analog output signal was around 500 mV peak-to-peak. The signal was attenuated by 18-dB, then amplified 24-dB (SHF-807). The resulting 1-volt (p-p) output was connected to a distributed feedback laser biased at 33 mA. After transmission over 20-km SSMF, a variable optical attenuator (VOA) was used to adjust the output optical power, followed by a 16-GHz photodetector (DSC-40S) to convert optical signals to electrical signals, which were then sampled by a real-time Digital Storage Oscilloscope (DSO-X92804A) with an 80-GS/s sampling rate. Finally, the captured samples were analysed by off-line DSP in MATLAB.

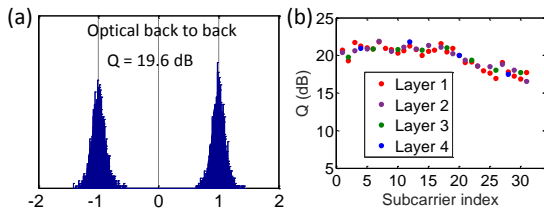


Fig. 5: Histograms and Q-factors for optical back-to-back.

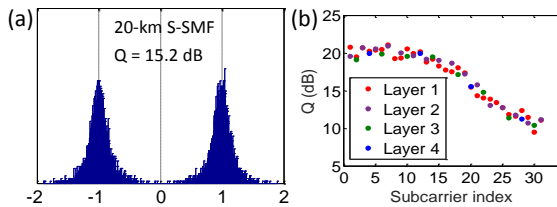


Fig. 6: Histograms and Q-factors for 20-km transmission

Firstly the optical back-to-back Q-factor was measured by directly connecting the laser output to the VOA set for zero attenuation. As shown in Fig. 5, the average Q-factor was 19.6 dB. There is a 5-dB penalty for the highest-frequency subcarriers, due to the limited laser bandwidth (small-signal resonance at 4 GHz for 33 mA). The iterative receiver substantially cancelled the clipping distortion from the lower layers to reveal the higher layers, evidenced by the Q-factors for a similar frequency being almost the same (some Q-factors for the same frequency indeed overlapped). Secondly, the Q-factor was evaluated after transmission over a 20-km span of SSMF, without optical amplification. The Q-factor calculated from the average BER is 15.2 dB (Fig. 6). Note, however, that the higher-index subcarriers suffer a 12-dB penalty, compared

with the low-frequency subcarriers, because of the interaction of laser chirp and fibre dispersion.

Conclusions

In this paper, an efficient real-time FPGA-based ASE-DMT transmitter with a net data rate of 9.2 Gb/s has been demonstrated. ASE-DMT usually requires one IFFT per layer, we show that only one IFFT module is required in the transmitter to generate all of the Layers, which then are clipped and added. With off-line signal processing in the receiver, the ASE-DMT signals are successfully transmitted over 20-km SSMF with a Q-factor higher than 15 dB, suggesting that higher data rates are possible through PAM-4.

Acknowledgements

This work is supported under the Australian Research Council's Laureate Fellowship (FL130100041) scheme.

References

- [1] M. H. Eiselt *et al.*, "Direct detection solutions for 100G and beyond," Proc. OFC, Tu3I.3, Los Angeles (2017).
- [2] L. Zhang *et al.*, "Beyond 100-Gb/s transmission over 80-km SMF using direct-detection SSB-DMT at C-band," J. Lightw. Technol., vol. **34**, pp. 723-729 (2016).
- [3] J. Armstrong and A. J. Lowery, "Power efficient optical OFDM," Electron. Lett., Vol. **42**, pp. 370-372 (2006).
- [4] S. C. J. Lee *et al.*, "PAM-DMT for intensity-modulated and direct-detection optical communication systems," Photon. Technol. Lett., Vol. **21**, pp. 1749-1751 (2009).
- [5] L. Chen *et al.*, "Successive decoding of anti-periodic OFDM signals in IM/DD optical channel," Proc. ICC, pp. 1-6 (2010).
- [6] Q. Wang *et al.*, "Layered ACO-OFDM for intensity-modulated direct-detection optical wireless transmission," Opt. Exp., Vol. **23**, pp. 12382-12393 (2015).
- [7] A. J. Lowery, "Comparisons of spectrally-enhanced asymmetrically-clipped optical OFDM systems," Opt. Exp., Vol. **24**, pp. 3950-3966 (2016).
- [8] M. S. Islam *et al.*, "On the superposition modulation for OFDM-based optical wireless communication," Proc. GlobalSIP, pp. 1022-1026 (2015).
- [9] M. S. Islam, and H. Haas, "Augmenting the spectral efficiency of enhanced PAM-DMT-based optical wireless communications," Opt. Exp., Vol. **24**, pp. 11932-11949 (2016).
- [10] B. Song *et al.*, "Experimental layered/enhanced ACO-OFDM short-haul optical fiber link," Photon. Technol. Lett., Vol. **28**, pp. 2815-2818 (2016).
- [11] Q. Wang *et al.*, "FPGA-based layered/enhanced ACO-OFDM transmitter," Proc. OFC, Tu3D-6 (2017).
- [12] Q. Wang *et al.*, "Hardware-efficient signal generation of layered/enhanced ACO-OFDM for short-haul fiber-optic links," submitted to Opt. Express.
- [13] H. Sorensen *et al.*, "Real-valued fast Fourier transform algorithms," IEEE Trans. Acoustics, Speech, and Signal Proc., Vol. **35**, pp. 849-863 (1987).